physica pss status solidi b

www.pss-b.com

basic solid state physics

Evolution of physical properties of conjugated systems

Wun-Fan Li[1], Marcin Andrzejak[,1], and Henryk A. Witek[*,1,2]**

[1] Institute of Molecular Science, National Chiao Tung University, 1001 Ta Hsueh Road, 30010 Hsinchu, Taiwan
[2] Department of Applied Chemistry, National Chiao Tung University, 1001 Ta Hsueh Road, 30010 Hsinchu, Taiwan

* Corresponding author: e-mail hwitek@mail.nctu.edu.tw, Phone: +886 35712121, ext: 56583, Fax: +886 35723764
**On leave from Faculty of Chemistry, Jagiellonian University, Krakow, Poland

Evolution of various physical properties of finite conjugated systems with increasing molecular size is studied using the self-consistent-charge density-functional tight-binding (SCC-DFTB) method. We usually observe a transition from the finite to the infinite regime for surprisingly short molecular chains containing only 20–30 monomer units of *cis*-butadiene, cyclopentadiene, pyrrole, furan, and thiophene. Such a fast convergence of equilibrium geometries, induced atomic charges, electron densities of states (DOS) and energy gaps, dipole and quadrupole moments, and polarizabilities is particularly striking considering the presence of strong π-conjugation.
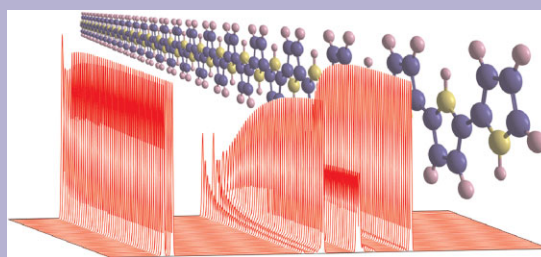
Convergence in the size evolution of majority of molecular properties of conjugated systems occurs for surprisingly short molecular chains.

1 Introduction The main idea of this study is to investigate the rate of convergence in the evolution of various physical properties of π-conjugated oligomers with the increasing length of the system. In the limit of an infinite chain, the studied systems converge toward polymers. Thus, it would be natural to think that also the properties of the finite oligomers should converge toward those of the polymers. This concept is a foundation of the so-called "oligomer approach" [1–11] used for experimental and theoretical determination of properties of infinite polymers. A natural, theoretical alternative to the oligomer approach are the usual techniques of solid-state physics dealing with infinite systems equipped with translational symmetry. Both of these methodologies were used in a number of studies to investigate a variety of physical properties of extended systems ([11–43], to cite only a few). However, none of these publications was fully devoted to a systematic analysis of the rate of convergence of the aforementioned properties. Here, to investigate the evolution, we explicitly consider oligomers

built of the following *trans*-connected monomers: *cis*-1,3-butadiene, cyclopentadiene, pyrrole, furan, and thiophene. In principle, two mesomeric forms are possible for the studied systems, aromatic and quinoid (or *trans*-cisoid and *cis*-transoid, respectively) [20, 44], which differ by the relative position of double bonds in the carbon backbone. Since it was demonstrated [40] that the former structure is substantially lower in energy, we consider only the aromatic-like oligomers and polymers. Note that the resulting infinite structure obtained from *cis*-1,3-butadiene is distinct from that one of all-*trans*-cisoid polyacetylene that was studied previously [34, 45, 46]. We focus on the rate of convergence of the following physical properties: equilibrium structures, HOMO–LUMO energy gaps, electronic densities of states, distributions of Mulliken charges, dipole and quadrupole moments, and polarizabilities. Our main interest lies in determining how rapidly the aforementioned properties saturate towards a constant value in the interior of the oligomers. Also, we want to find out the minimum length of

Original

Paper

Phys. Status Solidi B **249**, No. 2 (2012)   307

the oligomer chain for which the properties are indistinguishable from those of a given polymer. Selected properties of the systems studied here were already investigated either theoretically or experimentally in a number of studies. A complete review of these studies is out of scope of the present work. However, the concise compilation of references given here for the polymers and oligomers built of the acetylene [33, 46–49], cyclopentadiene [18, 19, 32, 33, 44, 48], pyrrole [12, 19, 23, 32–35, 42, 43, 48, 50–53], furan [19, 32–35, 42, 48, 50, 52], and thiophene [19, 32–35, 42–44, 48, 52, 54, 55] units is supposed to give a representative sample.

The theoretical tool used for our analysis is based on the self-consistent-charge density-functional tight-binding (SCC-DFTB) method [56–59], which can be considered as a simplified version of density functional theory (DFT). The SCC-DFTB energy expression is derived as a second-order Taylor expansion of the DFT energy with respect to density fluctuations. It has been extensively tested on various types of carbon-containing compounds showing that the reaction energetics, equilibrium geometries, and vibrational frequencies can be reproduced with accuracy comparable to DFT for a wide group of molecules including hydrocarbons, fullerenes, nanotubes, and small organic molecules [57, 60–64]. Using SCC-DFTB gives us the advantage of investigating extended molecular systems necessary to study the evolution of properties, which converge only in the limit of very large oligomers containing hundreds of atoms. An argument in favor of using SCC-DFTB for the analysis of π-conjugated systems is the successful application of this method in studying analogous properties of finite and infinite linear carbon chains [65]. A comparison with experimental and more advanced theoretical results demonstrated good performance of the approximate approach, which was successfully used in our group for a number of interesting applications [66–75]. Another very important advantage of using the SCC-DFTB method for our investigation is the possibility of a direct comparison with the analogous solid-state results. It should be stressed that we use here the same SCC-DFTB Hamiltonian within the frameworks of both quantum chemical and solid-state machineries. Thus, the solid-state calculations provide us with an excellent benchmark for the evolution of physical properties in oligomers.

2 Computational details We have considered explicitly five families of one-dimensional polymers: trans-cisoid polyacetylene, polycyclopentadiene, polyfuran, polypyrrole, and polythiophene. The size of the corresponding finite oligomers has varied from a single monomer ($m = 1$) unit to 50 monomer units ($m = 50$). The heavy-atom backbones of the models used in this study are planar. Vibrational analysis has shown that this is indeed their equilibrium geometry. A schematic geometrical representation of the studied systems is shown in Fig. 1. In addition to the quantum chemical calculations for the finite oligomers, we have performed calculations for the infinite polymer chains ($m = \infty$) using a standard solid-state SCC-DFTB approach. The unit cell used in these calculations – shown in Fig. 1 in square brackets – is
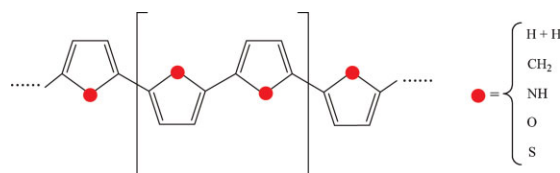

Figure 1 (online color at: www.pss-b.com) Schematic representation of the structure of the investigated oligomers. The square brackets depict the unit cell used in the solid-state calculations.

composed of two monomer units. Weak interchain interactions, structural defects, and dielectric shielding effects present in real three-dimensional crystals have been neglected. We believe, however, that these effects are not dominant and our models are still closely related to experimentally investigated structures.

The geometry optimization and energy calculations have been performed using a FORTRAN-based SCC-DFTB code developed by Porezag and co-authors [56]. The force convergence criterion for geometrical optimization is 10^{-7} a.u. and the SCC convergence threshold is 10^{-12} hartree. For the solid state calculations, the DFTB+ program [76] has been used. For each system, the initial unit cell structure has been extracted from the central region of the longest studied finite oligomers (50-mer). The lattice vectors perpendicular to the main axis of each polymer have been set to 100 Å to simulate a quasi-one-dimensional periodic structure. The positions of atoms within the initial unit cell and the remaining lattice constant a have been optimized (with 500 k-points) to yield a structure corresponding to minimal energy. After obtaining the equilibrium geometry of the unit cells, we have used 500 k-points between 0 and π/a to sample the band structure of each 1D polymer and to construct the electronic density of states (DOS) plots.

3 Results and discussion

3.1 Evolution of equilibrium structures We have computed equilibrium SCC-DFTB geometry for a series of finite oligomers built of *cis*-butadiene, cyclopentadiene, furan, pyrrole, and thiophene. The distribution of equilibrium bond lengths for the infinite polymers (solid black line) and for the longest studied oligomers (solid red line) is shown in Fig. 2. It is clear that both distributions are almost identical for all the considered systems. The only difference concerns a few small peaks associated with the terminal monomers. A brief inspection of Fig. 3 shows that the relative magnitude of these "terminal" peaks decays with the growing length of the oligomer and that in the limit of an infinite number of the monomer units each family of the distributions shown in Fig. 2 would be identical. This observation gives us the first important conclusion of this study, which states that the equilibrium geometry of an infinite system can be accurately accessed using the corresponding finite-length model. A natural question arising from this observation is how long the oligomer chain
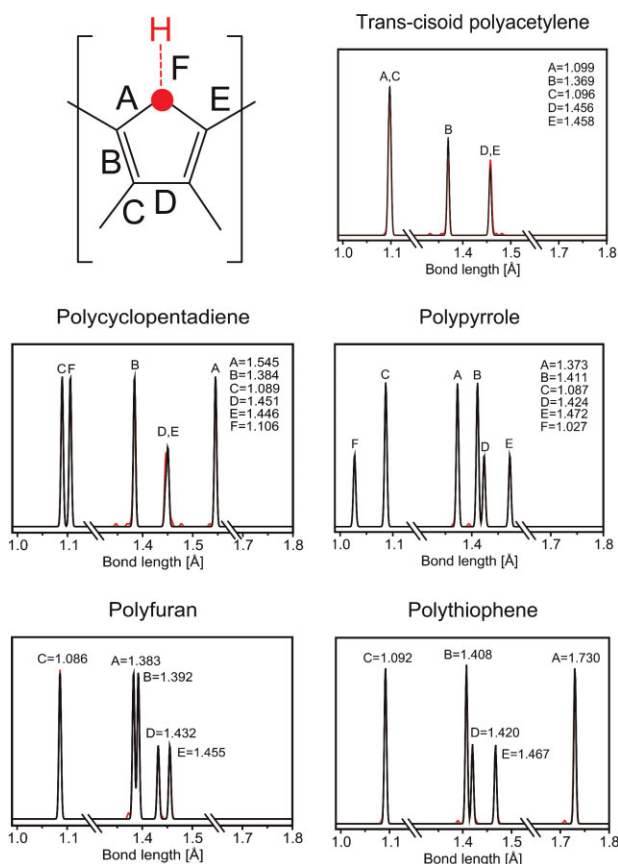
Figure 2 (online color at: www.pss-b.com) Bond length distributions for the studied systems. Black line represents the distribution obtained from the solid-state calculations and the red line, analogous distribution for longest studied oligomer (50-mer). Note that the two distributions almost perfectly overlap.

Figure 3 (online color at: www.pss-b.com) Convergence of the bond length distributions for the studied oligomers.

should be to reproduce the geometric parameters of the polymer. Figure 2 shows that 50-mers are more than sufficient for this purpose. In fact, Figs. 3 and 4 demonstrate that convergence of the equilibrium bond lengths and angles is obtained much faster; they reach the bulk limit for approximately 15–20 monomer units. The most dramatic changes in molecular geometry are observed for very short oligomer chains ($m = 1$–10). Our results demonstrate that such short chains should not be used for modeling the properties of polymers. However, the analysis of the presented data suggests that already a 20-mer makes an adequate geometrical model of an infinite polymer chain (for details see Section 4 and Table 3). Since the differences in the bond distributions for the finite and infinite systems come mainly from the effect of the terminal units, we have investigated in detail the behavior of selected bond lengths and bond angles as a function of their position in the chain, using the finite 50-mer of pyrrole as a representative of all the systems under study. The results are presented in Fig. 4 for two bond lengths and two bond angles. The results are more than surprising; they show that the effect of the finite termination is very local and is limited only to the 3–4
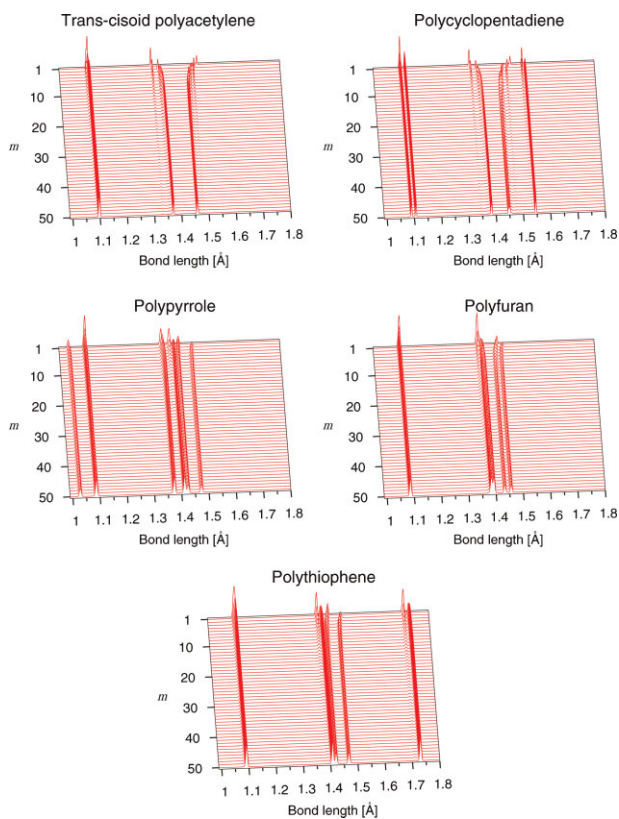
monomers adjacent to the terminal unit. To highlight this effect, we have also plotted in Fig. 4 the limit value obtained from the corresponding solid state calculations. The whole interior of the 50-mer of pyrrole is virtually identical to the structure of the infinite polymer. The effect of finite termination is limited only to a few terminal units, regardless of the length and type of the studied model. This observation gives us the second important conclusion of this study, which states that the equilibrium structure of the infinite polymer chain can be obtained by inspecting the interior of relatively short oligomer chains built of approximately 20 monomer units.

3.2 Evolution of HOMO–LUMO energy gaps
Experimental and theoretical investigations of the energy gaps of conjugated polymers via the analysis of the HOMO–LUMO gaps of a series of finite oligomers received considerable attention [33, 35, 40, 42, 44, 48, 77]. The computed HOMO–LUMO gaps for the five families of studied oligomers are presented in Fig. 5. The convergence of the HOMO–LUMO gaps towards the corresponding polymer band gaps seems very fast. However, closer scrutiny of Fig. 5 shows that the actual behavior is more complex. For oligomers of certain length, the HOMO–LUMO energy gap dependence on the reciprocal of the number of monomers m slowly begins to change from linear to quadratic [41].

Original

Paper

Phys. Status Solidi B **249**, No. 2 (2012)   309

Figure 5 (online color at: www.pss-b.com) HOMO–LUMO gaps of the oligomers as a function of the reciprocal of the chain length. The inset gives the extrapolated $m \rightarrow \infty$ values obtained from the second-order polynomial fit. Note that the ten shortest oligomers are excluded from the fit.
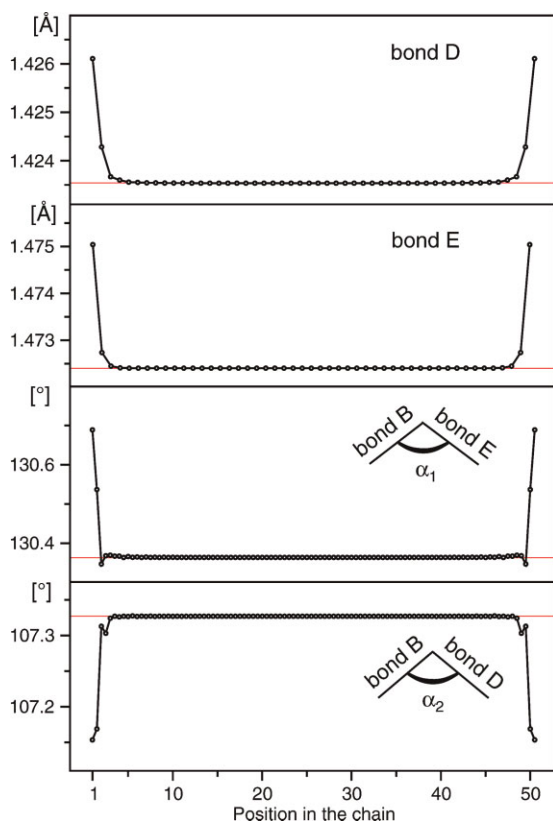
Figure 4 (online color at: www.pss-b.com) Selected bond lengths and bond angles as a function of the position in the chain of the 50-mer of polypyrrole. Thin solid line represents the corresponding values for the polymer, obtained from the solid-state calculations.

serious inaccuracies in a number of the reported polymer band gaps, obtained by applying the linear extrapolation procedure to the oligomer results [12]. Our estimates of the band gaps for the systems under study, using a quadratic fit for the longest 40 structures (so that the linear region is avoided) yields values almost identical to the actual energy gaps in infinite polymers obtained from the solid state SCC-DFTB calculations. The convergence of the HOMO–LUMO gaps for oligomers toward the band gaps of the corresponding polymers is demonstrated in Table 1. Note that for the longest studied finite chains, the HOMO–LUMO gap itself constitutes a good estimate of the value that can be obtained from the analogous solid-state calculations.

3.3 Evolution of electronic DOS distributions
The electronic density of states (DOS) is defined in solid state physics as an integral of one-electron energy levels over the Brillouin zone. In practice, however, only a finite number of Brillouin zone's points are sampled and the electronic DOS

Deviations from the linear trend are initially very subtle and one has to study quite long oligomers (20-mers, 30-mers, or even longer) to obtain a distinct quadratic dependence allowing for the proper (quadratic) extrapolation procedure [35]. The slow change in the nature of dependence the HOMO–LUMO gap with respect to $1/m$ was the source of
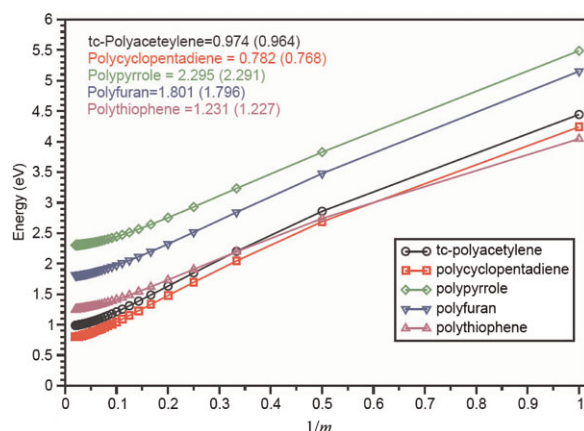
Table 1 HOMO–LUMO gaps [eV] of selected oligomers and the band gaps of the corresponding polymers. The relative error is computed with respect to the solid-state SCC-DFTB result.

	HOMO–LUMO gaps									
	tc-PA		PCp		PPy		PFu		PTh	
	value	error (%)	value	error (%)	value	error (%)	value	error (%)	value	error (%)
10-mer	1.211	24.3	1.045	33.6	2.444	6.5	1.975	9.7	1.412	14.7
20-mer	1.046	7.4	0.865	10.6	2.337	1.8	1.851	2.8	1.292	5.0
30-mer	1.008	3.5	0.821	5.0	2.314	0.8	1.824	1.3	1.264	2.7
40-mer	0.994	2.1	0.805	2.9	2.306	0.5	1.814	0.7	1.252	1.7
50-mer	0.987	1.3	0.797	1.9	2.302	0.3	1.81	0.5	1.247	1.3
polymer extrapolated	0.964	1.0	0.768	1.8	2.291	0.2	1.796	0.3	1.227	0.3
solid-state	0.974		0.782		2.295		1.801		1.231	
exp. [reference]	1.5	[11]			2.85	[12]	2.35	[15]	1.8	[78]

is obtained as a superposition of a finite number of the discrete energy levels. To ensure smooth character of DOS constructed in such a way, the discrete energy levels are usually smeared out using a Gaussian envelope of constant width (sometimes referred to as the relaxational broadening [23]). The equivalence of these two procedures in the limit of large number of sampling points suggests that the electronic DOSs can be also constructed using the set of discrete one-electron energy levels (i.e., orbital energies) of finite oligomers. This idea was used by Salzner et al. [32] to show in a qualitative way that the orbital levels of oligomers develop in the infinite limit into the band structures of the corresponding polymers. We have further tested this hypothesis in a quantitative way by plotting the resulting – finite and infinite – electronic densities of states in Fig. 6. Since SCC-DFTB employs minimal atomic basis sets, it is only meaningful to analyze the resulting DOSs around the Fermi level. To facilitate the analysis of these graphs, the peaks corresponding to the occupied energy levels (valence band) have shaded area, while those corresponding to the virtual energy levels (conductance band) are depicted with a solid line. The electronic DOSs for finite oligomers presented in Fig. 6 show a surprisingly fast convergence toward the infinite limit. Already for less than 10 monomer units, the finite DOSs are very similar to the one of the
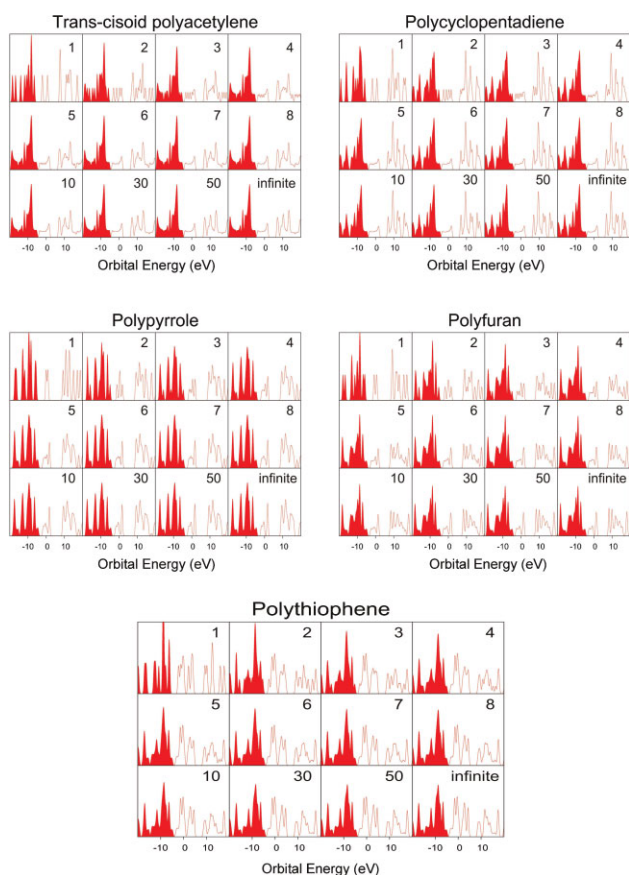
polymer. The electronic DOSs for the longest studied oligomers ($m = 50$) are practically indistinguishable from those obtained in the solid state calculations. Similar observation was previously made for polypyrrole [23], for which the DOS for oligomers built of six monomer units and the DOS for the corresponding polymer were closely related. Note that for each of our finite length oligomers, there are some tiny additional peaks present in every DOS. These spurious peaks correspond to the energy levels of the terminal hydrogen atoms. Obviously, the relative magnitude of these peaks decreases with the growing size of the chain and it is reduced to zero in the infinite limit.

3.4 Evolution of charge distribution Another important molecular quantity studied in this work is the electronic charge distribution. The induced atomic charges are computed using the Mulliken population analysis. First we discuss the distribution of the Mulliken charges along the longest studied oligomer chains. Figure 7 shows the Mulliken charges on the heteroatoms. The most striking feature is nearly instantaneous convergence of the Mulliken charge to the bulk value. The effect of the chain boundaries is visible only at the two terminal monomers. All the remaining monomers have virtually the same Mulliken charge as the infinite polymer. Figure 8 shows the change of Mulliken charges along the π-conjugated chains of carbon atoms. The C_{2v} symmetry of the monomer units implies the presence of
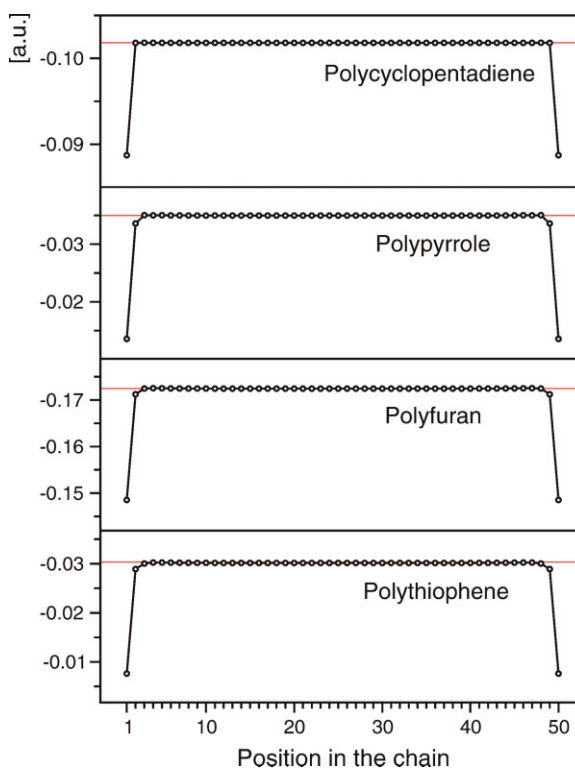

Figure 6 (online color at: www.pss-b.com) Convergence of the electronic DOS for all the considered models.

Figure 7 (online color at: www.pss-b.com) Mulliken charge on the heteroatom (or carbon of the CH$_2$ group) as a function of the position in the chain for the studied 50-mers. The corresponding solid-state values are depicted with thin red line.
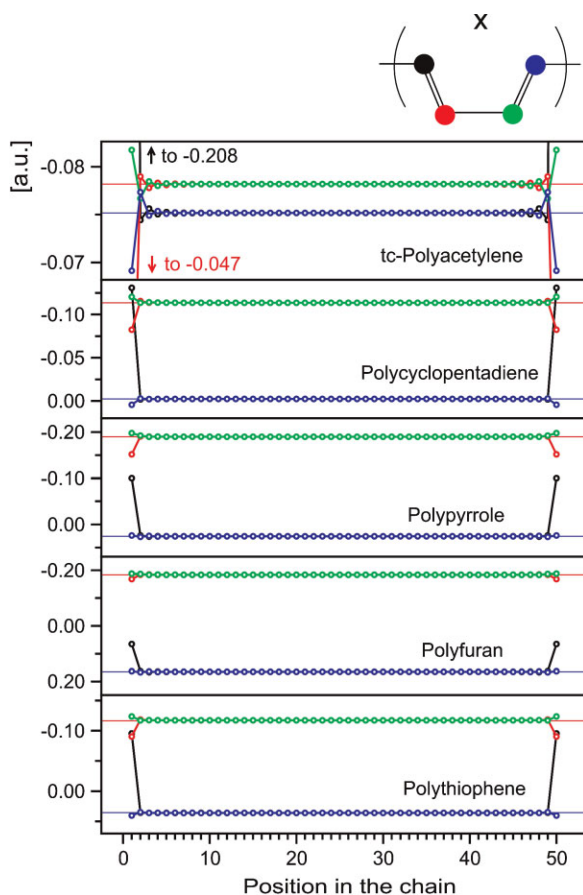
Original

Paper

Phys. Status Solidi B **249**, No. 2 (2012)

311

Figure 8 (online color at: www.pss-b.com) Mulliken charges on the carbon atoms as a function of their position in the conjugated oligomer backbone of the studied 50-mers. The corresponding solid-state values are depicted with thin red and blue lines. Note that each carbon atom within a monomer is depicted with a different color.

Figure 9 (online color at: www.pss-b.com) Mulliken charge on the nitrogen atom as a function of the position in the chain for the selected pyrrole oligomers. The corresponding solid-state value is depicted with thin red line.

two pairs of carbons with identical charges, C_α (blue and black) and C_β (green and red), as defined in Fig. 8. The symmetry enforces the same behavior in the corresponding, infinite polymer chains. Therefore, we expect that similar behavior can be also observed for the finite oligomers. Analysis of Fig. 8 shows that such a symmetry charge distribution is indeed observed in oligomers, as long as a given monomer is not located too close to the chain boundary. The charges at the two–three terminal units deviate from the values calculated for the corresponding polymers, but the charges at all the remaining monomers are virtually indistinguishable from those in polymers. Again, the rate with which the charges reach the bulk value is quite striking.

Eventually, let us inspect the evolution of the Mulliken charges with the elongation of the oligomer chain. The detailed analysis performed above for the 50-mers reveals that the Mulliken charges reach constant values already very close to the boundaries of the finite oligomers. This suggests that the interior of the chain will not be affected even after substantial reduction of the chain length. The illustration of
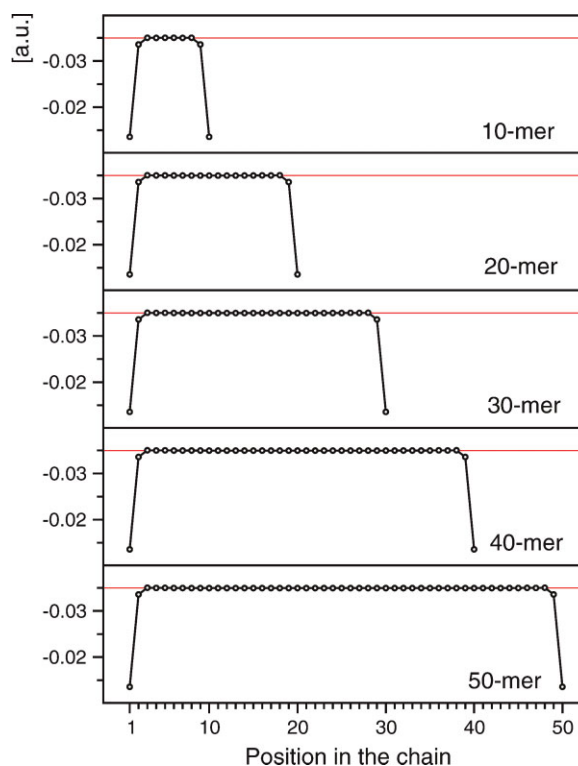
such a behavior is given in Fig. 9, which shows the distribution of the Mulliken charge on the nitrogen atoms in a series of finite oligopyrroles. The nature of the chain interior is preserved even in the 10-mer, which is a little surprising since the central part of such a short chain might be expected to "remember" its molecular origin. The presented results show, however, that the evolution of the Mulliken charges with the elongation of the oligomer chain is one of the most rapidly convergent properties among those studied in this work.

3.5 Evolution of dipole moments The oligomers built of an even number of monomers possess an inversion center (see Fig. 1) and therefore do not have any dipole moment. The situation is quite different for the oligomers with an odd value of m. The dipole moment in each of the considered monomers is oriented along the C_2 symmetry axis. Adding another monomer results in another identical dipole oriented along the same direction but with the opposite sign. It is clear that in a dimer – and analogously also in longer oligomers with even m – these two dipoles cancel out yielding a non-polar molecule, which is consistent with the presence of the inversion center. In oligomers with odd m complete cancellation is impossible. A short reflection on the value of the dipole moment in oligomers with odd m shows that it should be comparable in magnitude to the
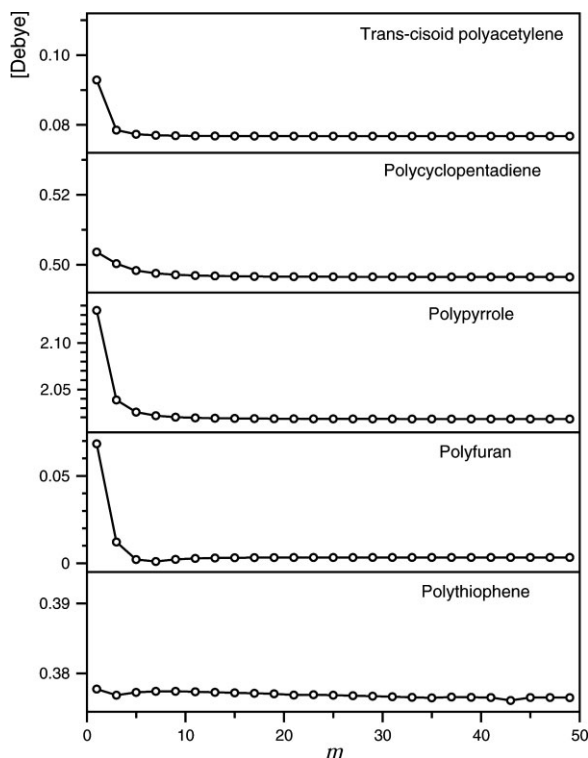
Figure 10 Magnitude of the dipole moment of the odd-m oligomers. Note that for all the even-m oligomers, and for the polymer, the dipole moment vanishes due to symmetry reasons.

Figure 11 (online color at: www.pss-b.com) Evolution of the quadrupole moment components (normalized per monomer unit) with growing length of the oligomer chain.

dipole of a monomer. We have plotted the absolute values of the dipole moments as a function of m in Fig. 10. The presented plots look very much alike. The dipole moment is reduced upon the elongation of the chain by 0.01–0.15 D. This change is the most pronounced for short chains. For chains longer than 11 monomer units, the absolute value of the dipole moment is practically constant. These results show that the modulus of the dipole moment is a rapidly converging molecular property and the bulk value is obtained already for $m > 11$.

3.6 Evolution of quadrupole moments The molecular quadrupole moment (QM) is a symmetric second rank tensor with six independent components [79]. Within the SCC-DFTB formalism, the QM tensor Θ is defined via a discrete summation over the Mulliken atomic charges

$$\Theta_{ij} = \sum_{A}^{atoms} \Delta q^A r_i^A r_j^A,$$

where Δq^A is the induced Mulliken charge on atom A and r_i^A and r_j^A are the Cartesian coordinates of the atom A. Note that owing to the discrete character of the charge distribution in the SCC-DFTB formalism, all the components of Θ related to the z coordinate – i.e., the coordinate perpendicular to the plane of the studied molecules – are identically equal to zero for all the studied systems except for polycyclopentadiene.
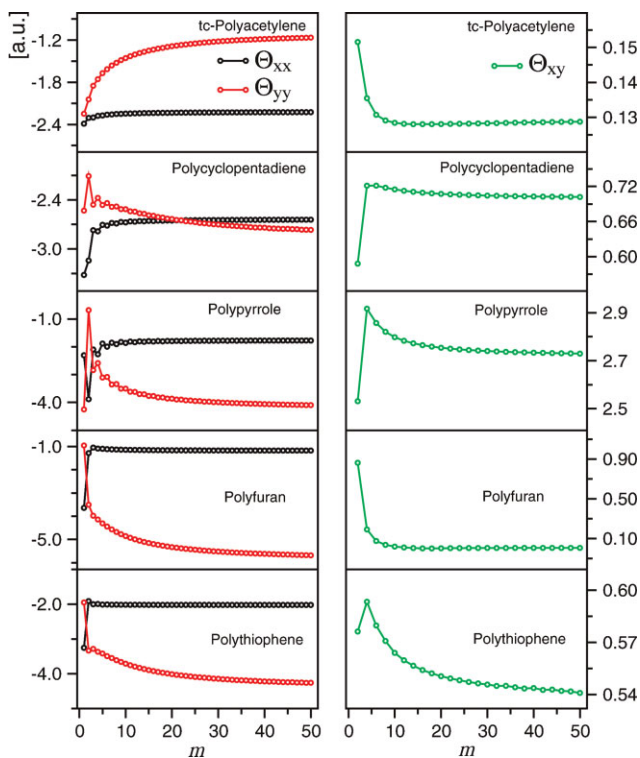
Therefore, it is sufficient to investigate the evolution of the tensor components related to the products of the x and y coordinates only. Moreover, for the molecules possessing the C_{2v} point group symmetry, i.e., for all the oligomers built of odd number of monomers, it is required for symmetry reasons that $\Theta_{xy} = 0$. It is assumed that the x and y are the in-plane molecular axes with the y-axis coinciding with the I_{min} principal axis of tensor of inertia.

The components of the QM tensor grow with the length of the investigated oligomers. To facilitate the comparison of this property for systems of different sizes, in Fig. 11 we show Θ_{xx}, Θ_{yy}, and Θ_{xy} normalized per monomer unit. The reduced tensor components seem to approach constant values; this suggests that the dependence of the QM tensor components on size of the system may become linear for sufficiently long oligomers. The convergence toward linearity is more pronounced and seemingly faster for Θ_{xx} than for Θ_{yy}. The result for Θ_{xx} is not surprising, since its linear growth is a simple consequence of an increasing number of repetitive units. More complicated mechanism seems to be responsible for the relatively slow convergence of Θ_{yy} and Θ_{xy}. Simple pictures based on physical intuition fail to explain the dependence as the QM tensor components result from a delicate balance originating from a cancellation of a large number of similar terms. Another rather surprising observation for even-m oligomers is a significant discrepancy between the relative orientations of the principal axes

Phys. Status Solidi B **249**, No. 2 (2012)

313

of the tensor of inertia and the principal axes of the QM tensor. For these systems, the molecular point group (C_{2h}) does not determine any particular directions in the xy plane. Taking into account strong geometrical asymmetry of the molecule and the interpretation of quadrupole moment as a measure of deviations of the charge distribution from sphericity, one might expect that the principal axes of both tensors would be similarly oriented. However, our calculations show that this is not the case. On one hand, the anisotropy of the tensor of inertia and the orientation of its principal axes are naturally rooted in the shape and size of the molecule. On the other hand, the molecular geometry does not seem to have a strong influence on the anisotropy and orientation of the quadrupole moment tensor. Even for the longest studied even-m oligomers, the in-plane principal axes of the QM tensor do not coincide with the corresponding principal axes of the tensor of inertia. The value of the angle between the long axes depends mainly on the type of heteroatom and varies from $0.08°$ for the 50-mer of furan to $42.46°$ for the 50-mer of cyclopentadiene. The signalized here unexpected characteristic of the quadrupole moment tensor calls for an extensive study of this property in extended conjugated systems.

3.7 Evolution of polarizabilities The molecular polarizability has been vigorously studied for a variety of extended conjugated systems [48, 50–52, 80–85]. Here, we analyze the trace and the anisotropy of the polarizability tensors

$$\langle \alpha \rangle = \frac{1}{3} \left(\alpha_{xx} + \alpha_{yy} + \alpha_{zz} \right),$$

$$\alpha_{\mathrm{ani}} = \sqrt{\frac{1}{2}\alpha_{\mathrm{A}} + 3\alpha_{\mathrm{B}}},$$

where

$$\alpha_{\mathrm{A}} = \left(\alpha_{xx} - \alpha_{yy} \right)^2 + \left(\alpha_{xx} - \alpha_{zz} \right)^2 + \left(\alpha_{yy} - \alpha_{zz} \right)^2,$$

$$\alpha_{\mathrm{B}} = \alpha_{xy}^2 + \alpha_{xz}^2 + \alpha_{yz}^2,$$

as these invariants are of direct, practical importance in theories of optoelectronics and intermolecular forces [86]. For the sake of clarity, we present these quantities as the values per monomer: $\langle \tilde{\alpha} \rangle = \langle \alpha \rangle / m$ and $\tilde{\alpha}_{\mathrm{ani}} = \alpha_{\mathrm{ani}} / m$. The renormalized invariants converge to constants when the additivity limit is reached. The results of our calculations are shown in Fig. 12. One can easily observe the convergent behavior of $\langle \tilde{\alpha} \rangle$ and $\tilde{\alpha}_{\mathrm{ani}}$. However, careful scrutiny of the graphs shows that saturation limits are not reached for any of the investigated systems. The convergence appears to be faster for the oligomers containing aromatic rings. In order to obtain saturated values of $\langle \tilde{\alpha} \rangle$ and $\tilde{\alpha}_{\mathrm{ani}}$, we adopt the
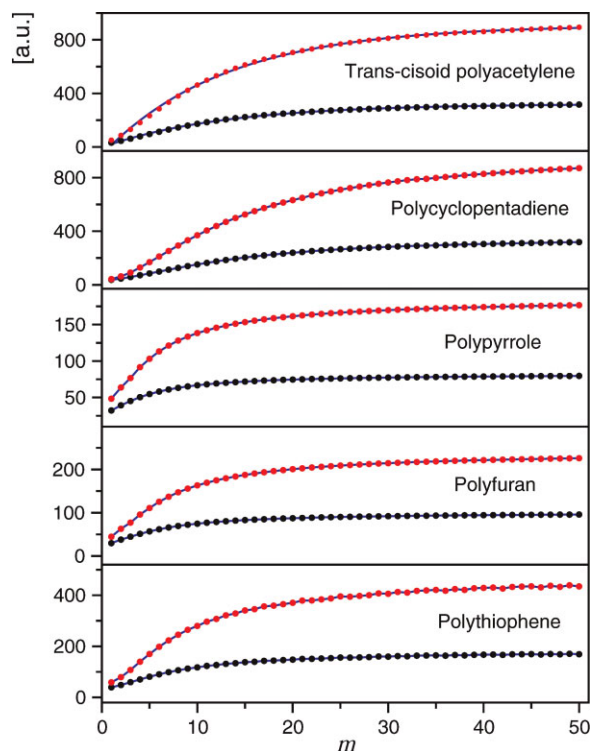

Figure 12 (online color at: www.pss-b.com) Evolution of the polarizability invariants (normalized per monomer unit) with growing length of the oligomer chain. Black color corresponds to the averaged polarizability, $\langle \tilde{\alpha} \rangle$, and the red color, to the polarizability anisotropy, $\tilde{\alpha}_{\mathrm{ani}}$. The analytical fits to the computed data are depicted using blue lines.

formula of Schulz et al. (Eq. (3.1) on page 455 in Ref. [82]):

$$\tilde{\alpha}_m = \tilde{\alpha}_\infty - c \cdot \exp \left(-\frac{m}{m_{\mathrm{sat}}} \right),$$

which was successfully applied for modeling the evolution of polarizabilities for conjugated oligomers [82] and carbon nanotubes [87]. Here, $\tilde{\alpha}_m$ denotes either of the polarizability invariants calculated for the m-unit oligomer, and $\tilde{\alpha}_\infty$ is an analogous quantity of the hypothetical infinite chain. In the ideal case, the prefactor c should be equal to $\tilde{\alpha}_\infty$ since for $m = 0$ the polarizability must vanish. However, by allowing c to vary, one can obtain a better fit to the calculated data, and consequently, a more accurate value of $\tilde{\alpha}_\infty$. The parameter m_{sat} is characteristic for a given type of oligomers; its large value indicates slow convergence of the polarizability invariants with growing m. The optimum parameters for all the studied oligomer systems are presented in Table 2.

In the context of the present study, one of the most important question is how long should the oligomer chain be to accurately reproduce the linear scaling of the polarizability invariants. By means of the formula given above and the fitted parameters, we have calculated the number of monomer units necessary for the polarizability invariants to

Table 2 The polarizability invariants [in a.u.] extrapolated to $m = \infty$. The effective conjugation length $m_{0.99}$ denotes the length of the oligomer chain, for which $\langle \tilde{\alpha} \rangle$ and $\tilde{\alpha}_{ani}$ reach 99% of their saturated values. For the meaning of the remaining parameters, see text.

		α_∞	c	m_{sat}	$m_{0.99}$
trans–cis-polyacetylene	$\langle \tilde{\alpha} \rangle$	322	324	13.0	60
	$\tilde{\alpha}_{ani}$	910	967	13.1	61
polycyclopentadiene	$\langle \tilde{\alpha} \rangle$	335	331	16.4	75
	$\tilde{\alpha}_{ani}$	922	987	16.7	78
polypyrrole	$\langle \tilde{\alpha} \rangle$	78	51	6.9	29
	$\tilde{\alpha}_{ani}$	174	141	7.5	33
polyfuran	$\langle \tilde{\alpha} \rangle$	94	72	8.0	35
	$\tilde{\alpha}_{ani}$	223	200	8.6	39
polythiophene	$\langle \tilde{\alpha} \rangle$	169	144	10.0	44
	$\tilde{\alpha}_{ani}$	435	424	10.3	47

reach 99% of their saturated values. This quantity – further referred to as $m_{0.99}$ – can be regarded as a good estimate of the π-electron delocalization along the oligomer chain. Evidently, the shortest chains for which the required accuracy is achieved are those corresponding to the pyrrole oligomers (29 monomer units) and the furan oligomers (35 monomer units). The convergence of $\langle \tilde{\alpha} \rangle$ is the slowest for the all-carbon oligomers, which require 60 and 75 monomer units for *trans–cis*-polyacetylene and *trans*-polycyclopentadiene, respectively, to obtain the necessary accuracy. Nevertheless, this analysis shows that the oligomer approach is essentially capable of reproducing the polymer polarizabilities, even though the convergence is much slower than for the geometry and charge related properties.

4 Conclusions We have studied the evolutions of geometry, electronic DOS and energy gaps, Mulliken atomic charges, dipole and quadrupole moments as well as polarizabilities for five series of linear oligomers containing from one to 50 monomer units. The monomers are *cis*-butadiene, cyclopentadiene, and three most common heterocyclic rings: furan, pyrrole, and thiophene. We have found that the majority of the studied properties show prominent convergence towards constant values regardless of the type of the heteroatom. Analysis of geometry and Mulliken charges of individual monomers along the chain has shown

that already for quite short chains (20-mers) the interior of the chain is virtually indistinguishable from the corresponding polymer, calculated at the same level of theory. Only several terminal units – about 3–4 for geometries and charges – display discernible deviations from the bulk values. Such a fast convergence of the geometric parameters as well as atomic charges is of great practical importance as it allows for investigating quasi-one-dimensional polymers using relatively small, molecular models. Similarly, the fast, convergent behavior of the electronic DOSs allows for theoretical insight into the electronic structure of semi-conductive polymers at the molecular level. This can be especially advantageous in studies of the energetics of the guest electronic levels introduced by doping a polymer with electron-deficient or electron-rich atoms or groups. In order to quantitatively reproduce the energy gap, one has to consider oligomers longer than those appropriate for studying geometry or charge related properties, since the convergence of the HOMO–LUMO gap with increasing chain length is considerably slower than the evolution of, e.g., charge distribution. Note that the computed SCC-DFTB band gaps are underestimated by 20–35% with respect to the experimental data; similar discrepancy is characteristic also for other DFT-based results [11].

Quadrupole moments and polarizabilities belong to the class of properties that show slower convergence towards the infinite limits. In fact, for the all-carbon oligomers, they have not reached the expected linear scaling behavior even for the longest monomers studied in this work. We have computed the minimal length of an oligomer, for which the polarizability per monomer is reproduced with error smaller than 1%; for details, see Table 3. The limiting number of units is the smallest for the oligomers containing the aromatic rings (29 for pyrrole and 35 for furan). The largest number of monomers necessary to achieve the required accuracy has been found for the non-aromatic *trans–cis*-polyacetylene and polycyclopentadiene (60 and 75, respectively), whereas the oligothiophenes (44 monomer units) can be regarded as an intermediate case. The computed numbers of monomers can be a rough estimation of the effective conjugation length in the studied systems. Premature disruption of the π-electron conjugation that takes place in short oligomer chains is the most likely cause of the slow convergence of the second (and higher) order tensor properties observed in this study.

Table 3 The number of monomer units required for a given property to reach the corresponding polymer value within the deviation of 1%. For bond lengths and dipole moments, the permitted deviations are set to 0.001 Å and 0.001 D, respectively.

	trans–cis-polyacetylene	polycyclopentadiene	polypyrrole	polyfuran	polythiophene
bond lengths	8	9	4	5	6
band gaps	56	59	24	34	44
DOS	21	28	22	31	19
charges	5	13	5	5	5
dipole moment	5	9	11	11	5
quadrupole moment	46	53	35	41	45
polarizability	61	78	33	39	47

Phys. Status Solidi B **249**, No. 2 (2012)

315

Original

Paper

The analysis of extended systems presented here shows that the oligomer approach is essentially capable of modeling molecular properties of polymers, even though the slow convergence of some of the properties requires using oligomers of considerable length. The SCC-DFTB methodology has proved to provide a consistent, semi-quantitative picture of the evolution of the oligomer properties. Even though the actual values of the computed parameters may be somewhat approximate, we believe that the conclusions presented here can be used as guidelines in other experimental and theoretical investigations of related systems.

References

[1] A. Karpfen and M. Kertesz, J. Phys. Chem. **95**, 7680 (1991).

[2] J. Cioslowski and M. B. Lepetit, J. Chem. Phys. **95**, 3536 (1991).

[3] S. Zalis and M. Kertesz, Synth. Met. **47**, 179 (1992).

[4] S. Y. Hong, Bull. Kor. Chem. Soc. **16**, 845 (1995).

[5] J. Cornil, D. Beljonne, and J. L. Bredas, Synth. Met. **85**, 1029 (1997).

[6] U. Salzner, P. G. Pickup, R. A. Poirier, and J. B. Lagowski, J. Phys. Chem. A **102**, 2572 (1998).

[7] S. Ramasesha, S. K. Pati, Z. Shuai, and J. L. Bredas, Adv. Quantum Chem. **38**, 121 (2000).

[8] O. Kwon and M. L. McKee, J. Phys. Chem. B **104**, 1686 (2000).

[9] M. Tachibana, S. Tanaka, Y. Yamashita, and K. Yoshizawa, J. Phys. Chem. B **106**, 3549 (2002).

[10] E. J. Weniger and B. Kirtman, Comp. Math. Appl. **45**, 189 (2003).

[11] S. J. Yang, P. Olishevski, and M. Kertesz, Synth. Met. **141**, 171 (2004).

[12] G. Zotti, S. Martina, G. Wegner, and A. D. Schluter, Adv. Mater. **4**, 798 (1992).

[13] T. C. Chung, J. H. Kaufman, A. J. Heeger, and F. Wudl, Phys. Rev. B **30**, 702 (1984).

[14] J. Roncali, A. Yassar, and F. Garnier, J. Chem. Soc. Chem. Comm. 581 (1988).

[15] S. Glenis, M. Benz, E. Legoff, J. L. Schindler, C. R. Kannewurf, and M. G. Kanatzidis, J. Am. Chem. Soc. **115**, 12519 (1993).

[16] V. Hernandez, J. T. L. Navarrete, and J. I. Marcos, Synth. Met. **41**, 789 (1991).

[17] M. Hissler, P. W. Dyer, and R. Reau, Coord. Chem. Rev. **244**, 1 (2003).

[18] S. Y. Hong and D. S. Marynick, Macromolecules **28**, 4991 (1995).

[19] S. Y. Hong, S. J. Kwon, S. C. Kim, and D. S. Marynick, Synth. Met. **69**, 701 (1995).

[20] S. Y. Hong, S. J. Kwon, and S. C. Kim, J. Chem. Phys. **103**, 1871 (1995).

[21] J. M. Toussaint and J. L. Bredas, Synth. Met. **69**, 637 (1995).

[22] J. L. Bredas, J. C. Scott, K. Yakushi, and G. B. Street, Phys. Rev. B **30**, 1023 (1984).

[23] W. K. Ford, C. B. Duke, and W. R. Salaneck, J. Chem. Phys. **77**, 5030 (1982).

[24] K. K. Kanazawa, A. F. Diaz, R. H. Geiss, W. D. Gill, J. F. Kwak, J. A. Logan, J. F. Rabolt, and G. B. Street, J. Chem. Soc. Chem. Commun. 854 (1979).

[25] S. Martina, V. Enkelmann, A. D. Schluter, G. Wegner, G. Zotti, and G. Zerbi, Synth. Met. **55**, 1096 (1993).

[26] G. Distefano, D. Jones, M. Guerra, L. Favaretto, A. Modelli, and G. Mengoli, J. Phys. Chem. **95**, 9746 (1991).

[27] M. J. Gonzalez-Tejera, E. S. de la Blanca, and I. Carrillo, Synth. Met. **158**, 165 (2008).

[28] A. Forni, M. Sironi, M. Raimondi, D. L. Cooper, and J. Gerratt, J. Phys. Chem. A **101**, 4437 (1997).

[29] M. Kobayashi, J. Chen, T. C. Chung, F. Moraes, A. J. Heeger, and F. Wudl, Synth. Met. **9**, 77 (1984).

[30] J. Roncali, Chem. Rev. **92**, 711 (1992).

[31] J. L. Bredas, R. Silbey, D. S. Boudreaux, and R. R. Chance, J. Am. Chem. Soc. **105**, 6555 (1983).

[32] U. Salzner, J. B. Lagowski, P. G. Pickup, and R. A. Poirier, Synth. Met. **96**, 177 (1998).

[33] J. Ma, S. H. Li, and Y. S. Jiang, Macromolecules **35**, 1109 (2002).

[34] A. K. Bakhshi, J. Ladik, and M. Seel, Phys. Rev. B **35**, 704 (1987).

[35] S. S. Zade and M. Bendikov, Org. Lett. **8**, 5243 (2006).

[36] U. Salzner, O. Karalti, and S. Durdagi, J. Mol. Model. **12**, 687 (2006).

[37] U. Salmer, Curr. Org. Chem. **8**, 569 (2004).

[38] J. Roncali, Chem. Rev. **97**, 173 (1997).

[39] R. E. Martin and F. Diederich, Ang. Chem. Int. Ed. **38**, 1350 (1999).

[40] M. Kertesz, C. H. Choi, and S. J. Yang, Chem. Rev. **105**, 3448 (2005).

[41] G. R. Hutchison, Y. J. Zhao, B. Delley, A. J. Freeman, M. A. Ratner, and T. J. Marks, Phys. Rev. B **68**, 035204 (2003).

[42] G. R. Hutchison, M. A. Ratner, and T. J. J. Marks, Phys. Chem. A **106**, 10596 (2002).

[43] J. L. Bredas, B. Themans, J. G. Fripiat, J. M. Andre, and R. R. Chance, Phys. Rev. B **29**, 6761 (1984).

[44] H. Subramanian and J. B. Lagowski, Int. J. Quantum Chem. **66**, 229 (1998).

[45] M. Springborg, Phys. Rev. B **33**, 8475 (1986).

[46] S. Hirata, H. Torii, and M. Tasumi, Bull. Chem. Soc. Jap. **69**, 3089 (1996).

[47] S. Hirata, H. Torii, and M. Tasumi, Phys. Rev. B **57**, 11994 (1998).

[48] D. Delaere, M. T. Nguyen, and L. G. Vanquickenborne, Phys. Chem. Chem. Phys. **4**, 1522 (2002).

[49] B. Champagne, E. A. Perpete, S. J. A. van Gisbergen, E. J. Baerends, J. G. Snijders, C. Soubra-Ghaoui, K. A. Robins, and B. Kirtman, J. Chem. Phys. **109**, 10489 (1998).

[50] P. Leiva, A. Martinez, and P. Otto, Synth. Met. **156**, 648 (2006).

[51] J. L. Toto, T. T. Toto, C. P. Demelo, and K. A. Robins, J. Chem. Phys. **102**, 8048 (1995).

[52] P. Otto, M. Piris, A. Martinez, and J. Ladik, Synth. Met. **141**, 277 (2004).

[53] G. Zerbi, M. Veronelli, S. Martina, A. D. Schluter, and G. Wegner, Adv. Mater. **6**, 385 (1994).

[54] S. S. Zade and M. Bendikov, Chem. Eur. J. **13**, 3688 (2007).

[55] J. W. van der Horst, P. A. Bobbert, M. A. J. Michels, G. Brocks, and P. J. Kelly, Phys. Rev. Lett. **83**, 4413 (1999).

[56] M. Elstner, D. Porezag, G. Jungnickel, J. Elsner, M. Haugk, T. Frauenheim, S. Suhai, and G. Seifert, Phys. Rev. B **58**, 7260 (1998).

[57] T. Frauenheim, G. Seifert, M. Elstner, Z. Hajnal, G. Jungnickel, D. Porezag, S. Suhai, and R. Scholz, Phys. Status Solidi B **217**, 41 (2000).

[58] H. A. Witek, S. Irle, and K. Morokuma, J. Chem. Phys. **121**, 5163 (2004).

[59] A. F. Oliveira, G. Seifert, T. Heine, and H. A. Duarte, J. Braz. Chem. Soc. **20**, 1193 (2009).

[60] H. A. Witek and K. Morokuma, J. Comput. Chem. **25**, 1858 (2004).

[61] E. Małolepsza, H. A. Witek, and K. Morokuma, Chem. Phys. Lett. **412**, 237 (2005).

[62] H. A. Witek, K. Morokuma, and A. Stradomska, J. Chem. Phys. **121**, 5171 (2004).

[63] H. A. Witek, K. Morokuma, and A. Stradomska, J. Theor. Comput. Chem. **4**, 639 (2005).

[64] A. Kuc, T. Heine, and G. Seifert, Phys. Rev. B **81**, 085430 (2010).

[65] C. P. Chou, W. F. Li, H. A. Witek, and M. Andrzejak, in: Spectroscopy, Dynamics, and Molecular Theory of Carbon Plasmas and Vapors, edited by L. Nemes and S. Irle (World Scientific, Singapore, 2011), pp. 417–444.

[66] X. Feng, S. Irle, H. A. Witek, K. Morokuma, R. Vidic, and E. Borguet, J. Am. Chem. Soc. **127**, 10533 (2005).

[67] H. A. Witek, S. Irle, G. Zheng, B. de Jong, and K. Morokuma, J. Chem. Phys. **125**, 214706 (2006).

[68] E. Małolepsza, H. A. Witek, and S. Irle, J. Phys. Chem. A **111**, 6649. (2007).

[69] G. Zheng, H. A. Witek, P. Bobadova-Parvanova, S. Irle, D. Musaev, R. Prabhakar, and K. Morokuma, J. Chem. Theory Comput. **3**, 1349 (2007).

[70] H. A. Witek, C. Koehler, T. Frauenheim, K. Morokuma, and M. Elstner, J. Phys. Chem. A **111**, 5712 (2007).

[71] H. A. Witek, B. Trzaskowski, E. Małolepsza, K. Morokuma, and L. Adamowicz, Chem. Phys. Lett. **446**, 87 (2007).

[72] E. Małolepsza, Y. P. Lee, H. A. Witek, S. Irle, C. F. Lin, and H. M. Hsieh, Int. J. Quantum Chem. **109**, 1999 (2009).

[73] M. Gaus, C. P. Chou, H. A. Witek, and M. Elstner, J. Phys. Chem. A **113**, 11866 (2009).

[74] W. Li, S. Irle, and H. A. Witek, ACS Nano **4**, 4475 (2010).

[75] D. V. Kazachkin, Y. Nishimura, H. A. Witek, S. Irle, and E. Borguet, J. Am. Chem. Soc. **129**, 8191 (2011).

[76] B. Aradi, B. Hourahine, and T. Frauenheim, J. Phys. Chem. A **111**, 5678 (2007).

[77] Y. S. Lee and M. Kertesz, J. Chem. Phys. **88**, 2609 (1988).

[78] K. Sakurai, H. Tachibana, N. Shiga, C. Terakura, M. Matsumoto, and Y. Tokura, Phys. Rev. B **56**, 9552 (1997).

[79] R. J. Doerksen and A. J. Thakkar, J. Phys. Chem. A **103**, 10009 (1999).

[80] M. T. Zhao, B. P. Singh, and P. N. Prasad, J. Chem. Phys. **89**, 5535 (1988).

[81] S. Kishino, Y. Ueno, K. Ochiai, M. Rikukawa, K. Sanui, T. Kobayashi, H. Kunugita, and K. Ema, Phys. Rev. B **58**, 13430 (1998).

[82] M. Schulz, S. Tretiak, V. Chernyak, and S. Mukamel, J. Am. Chem. Soc. **122**, 452 (2000).

[83] E. K. Dalskov, J. Oddershede, and D. M. Bishop, J. Chem. Phys. **108**, 2152 (1998).

[84] S. Tretiak, V. Chernyak, and S. Mukamel, Phys. Rev. Lett. **77**, 4656 (1996).

[85] F. Torrens, J. Sanchez-Marin, and I. Nebot-Gil, J. Mol. Struct. (Theochem) **426**, 105 (1998).

[86] A. Hinchliffe and H. J. Soscun, J. Mol. Struct. (Theochem) **331**, 109 (1995).

[87] L. Jensen, P. O. Astrand, and K. V. Mikkelsen, J. Phys. Chem. A **108**, 8795 (2004).